Publications of the Astronomical Society of Australia (PASA), Vol. 33, e057, 15 pages (2016).

doi:10.1017/pasa.2016.49

Relations Between He I λ10830 Absorption Strength and Stellar Activity Amongst Dwarf Stars

Graeme H. Smith[1,2]

[1]University of California Observatories and Department of Astronomy & Astrophysics, University of California, 1156 High Street, Santa Cruz, CA 95064, USA
[2]Email: graeme@ucolick.org

(Received July 30, 2016; Accepted October 11, 2016)

Abstract

Correlations are identified between the strength of the λ10830 He I triplet line and the following tracers of stellar activity amongst FGK dwarfs with colours of $(B-V) > 0.47$: coronal soft X-ray emission, emission in the λ1549 C IV and λ1335 C II lines originating from the transition region, and Ca II H and K emission from the chromosphere. No such correlations are present amongst dwarfs with spectral type earlier than F6. In addition, G and K dwarfs with strong triplet lines show evidence of excess flux in the *GALEX FUV* band compared to weak-triplet-line dwarfs. The X-ray spectra of late-F, G, and K dwarfs with He I triplets stronger than 160 mÅ have greater values of the *ROSAT* hardness ratio HR1 than are typical of weak-triplet dwarfs in the same range of spectral type. In other words, dwarfs later than F7V with strong He I triplet lines tend towards harder 0.1–2.0 keV X-ray spectra than weak-triplet dwarfs, although values of HR1 ~ -0.2 to $+0.1$ can still be encountered amongst a minority of weak-He-triplet stars. As regards, FGK main sequence stars the observational data on the λ10830 triplet line remains sparse. Progress could be made through spectroscopy of high resolution for samples of hundreds of stars, selected on the basis of having other measures of chromospheric and coronal activity available.

Keywords: stars: activity – stars chromospheres – stars: coronae – stars: late-type

1 INTRODUCTION

One of the few spectroscopic features formed by helium in the optical/near-infrared spectrum of late spectral type (F, G, K) dwarf stars is a triplet line at λ10 830 Å arising from the chromosphere. Although this is a relatively weak feature, it is one of the few He lines available for cool stars. The lower level of this triplet transition of ortho-helium is expected to be poorly populated at typical chromospheric temperatures, since this level is 20 eV above the ground state of neutral helium (Andretta & Jones 1997). So one issue with utilising this line has been understanding the mechanism by which electrons arrive in the lower level of the 10 830 Å triplet transitions (e.g., Athey & Johnson 1960; Andretta & Jones 1997; Centeno et al. 2008).

The He I triplet has been studied in spectroheliograms of the Sun where it is found that λ10830 absorption spatially traces the Hα network, He II λ304 resonance-line emission, and soft X-ray emission, which in turn trace active regions on the solar disk (Giovanelli, Hall, & Harvey 1972; Harvey & Sheeley 1977). Malanushenko & Jones (2005) found that coronal hole boundaries traced with λ10830 imaging spectroscopy are in accord with EUV imaging from the *SOHO* spacecraft, whilst de Toma et al. (2005) showed that EUV and X-ray dimmings on the solar disk are accompanied by λ10830 brightenings. Ground-based spatially resolved imaging in the λ10830 multiplet transition has now become a tool for tracing solar activity and dynamics in the corona, transition region (TR), and chromosphere (e.g., Lites et al. 1985; Harvey & Livingston 1994; Dupree, Penn, & Jones 1996; Zeng et al. 2014). With regard to theoretical studies, Avrett, Fontenla, & Loeser (1994), Andretta & Jones (1997), and Centeno et al. (2008) have shown from model calculations of the extended solar atmosphere that the intensity of the λ10830 He I triplet depends on EUV photons, capable of photoionising helium, that originate from the corona.

Zirin (1982), Smith (1983), and Zarro & Zirin (1986) extended the study of the He I λ10830 feature to other late-type dwarf stars. Zarro & Zirin (1986) found that for G and K dwarfs with $(B-V) > 0.5$ (spectral types of F7V and later) the equivalent width (EW) of the λ10830 feature correlates with the degree of coronal activity as quantified by the soft X-ray luminosity L_x/L_{bol}. They argued that this correlation is consistent with the lower state of the triplet transition being

populated by recombination of an electron with an He II ion, after the later has been produced via ionisation of He I by high-energy photons with wavelengths shortward of 504 Å (Zirin 1975), in accord with the above-noted solar modelling.

Sanz-Forcada & Dupree (2008) directly addressed the EUV-photon photoionisation-recombination (EUV-PR) model for the He I triplet line by high-resolution spectroscopy of the λ10830 feature of 15 stars (including both dwarfs and giants) for which observations from the *Extreme Ultraviolet Explorer* satellite were obtained. They derived the EUV luminosity in the wavelength range 80–170 Å. Their finding was that 'active dwarf and subgiant stars do not exhibit a relation between the EUV flux and the EW of the He I 10830 Å line'. On this basis, Sanz-Forcada & Dupree (2008) suggested that very active dwarf stars may have sufficiently high chromospheric and TR densities for collisional excitation to be more important than the EUV-PR mechanism for populating the lower level of the triplet transitions.

Whilst a small number of additional observational programmes aimed at the λ10830 He I feature amongst dwarf stars have appeared since the work of Zarro & Zirin (1986), there has been a notable increase in the amount of ancillary data pertaining to stellar activity amongst the dwarfs in their survey. Since correlations between λ10830 He I line strength and proxies for coronal region conditions have been a basis for testing models of λ10830 line formation, it seems worthwhile to return to the Zarro & Zirin (1986) sample of stars with a more extensive set of stellar activity data. A compilation has therefore been made of additional soft X-ray luminosities, hardness ratios, Ca II H and K emission line strengths, fluxes in the λ1549 C IV TR emission line, and photometry of the mid-UV spectrum, for the ∼70 dwarfs covered in the Zarro & Zirin (1986) paper. In addition, several more recent sources of He I data have been assimilated, in order to further document relationships between the strength of the λ10830 He I triplet and stellar activity for dwarf stars of F, G, and K spectral type.

2 DATA COMPILATION

Four sources of He I λ10830 EW data have been relied upon in this study, the predominant one being the work of Zarro & Zirin (1986; ZZ). The EW measures tabulated by them are mostly multiples of 25 mÅ, and the accuracy of their measurements is quoted as ≈ ±30 mÅ. Attention here is restricted to those stars listed under the 'Dwarfs' category in Zarro & Zirin's Table 1, although a small number of these stars have spectral types indicative of subgiants. Giants and supergiants observed by Zarro & Zirin (1986) are not considered, the focus of this paper being on dwarf stars. O'Brien & Lambert (1986) have made an extensive study of both the He I λ10830 strength and line profile amongst giant stars.

Additional sources that have been utilised for He I λ10830 EW data are Sanz-Forcada & Dupree (2008; SD), Takeda & Takada-Hidai (2011; TT), and Smith, Dupree, & Strader (2012; SDS). These references have led to the sample of dwarfs listed in Table 1 (stars from ZZ), additional Population I stars from SD and TT as listed in Table 2, and stars with metallicities of [Fe/H] ≤ −0.7 from TT and SDS which are compiled in Table 3. Many, but not all, stars in Table 3 are potentially Population II members of the Galactic halo, and as such are expected to be of greater age than stars in Tables 1 and 2. Uncertainties in the EW measurements are quoted as typically being 15% for Sanz-Forcada & Dupree (2008), and 20–30% for Takeda & Takada-Hidai (2011). Smith et al. (2012) did not quote formal uncertainties. In the case of stars HD 194598 and HD 201891, both of which were observed by TT and SDS, the agreement in λ10830 EW between these two papers is within 10 mÅ. The He I EWs have been used directly as they are given in the various sources, and no attempt has been made to apply any corrections between the different data sets.

There are six stars in common between the Table 1 sample of Zarro & Zirin (1986) and that of Table 2. Three of these stars have very strong He I triplet lines, and there are considerable differences in the EW values amongst the literature sources: HD 22049 (150 mÅ from Table 1 and 310 mÅ from Table 2), HD 98230 (295 mÅ and 380 mÅ), and HD 131156 (200 mÅ and 291 mÅ). In all three instances, the Zarro & Zirin values of EW are the smaller ones, and the differences range from 90–160 mÅ. It is possible that the He I triplet strength varies with time for such stars, since the differences in EW between the two literature sources are greater than the observational uncertainties. Considering the six stars that appear in both Tables 1 and 2, the mean difference in He I EW is 58 mÅ with a standard deviation of 71 mÅ. It is the observations of the three most-active dwarfs that dominate this difference, since for the three weaker-He dwarfs (HD 10700, HD 141004, and HD 161797), the mean difference in EW is only 4 mÅ with a standard deviation of 45 mÅ.

Tables 1–3 contain a variety of ancillary data for each star obtained from various sources in the literature. Values of V and $B-V$ were taken from The General Catalogue of Photometric Data (Mermilliod, Mermilliod, & Hauck 1997; GCPD). Metallicities listed in Table 3 are as quoted by TT and SDS. The column labelled Notes in each table gives information about various stars gleaned from the SIMBAD Astronomical Database (Wenger et al. 2000). All but one of the stars in Tables 1 and 2 are within 60 pc of the Sun.

Measures of coronal and chromospheric activity used in this paper take the form of soft X-ray luminosity, and emission in the H and K lines of the Ca II ion, respectively. The main source used for the former is the *ROSAT* spacecraft observatory (e.g., Voges et al. 1999), and for present purposes the soft X-ray luminosity relative to the bolometric luminosity was calculated. Ground-based measurements of the emission in the chromospheric components of the Ca II H and K lines are customarily presented in the literature in the form of an index $R'_{\rm HK}$, which is the ratio of the flux emitted in the H and K chromospheric emission features to the bolometric flux of a star (Noyes et al. 1984). The Ca II HK data have been obtained from a combination of published sources as

Table 1. Data for dwarf stars from Zarro & Zirin (1986).

HD	HeEW (mÅ)[b]	$\log(L_x/L_{bol})$	HR1[c]	$\log R'_{HK}$	V	$(B-V)$	$(m_{FUV}-B)$[d]	$c(19-27)$[e]	Notes[f]
432	200	−6.48	−0.55	....	2.268	0.341	....	0.79	δ Sct
3651	0	....	....	−4.95	5.877	0.851	13.04	....	var
8723	200	−5.08	−0.17	....	5.382	0.380	8.11	0.85	var
8774	200	−5.21	−0.42	....	6.283	0.450	9.25	0.70	...
9562	0	....	....	−5.13	5.757	0.639	11.84	....	...
10700	50	−6.21	−1.00	−4.97	3.495	0.727	....	....	...
11443	320	−4.80	−0.04	−4.35	3.416	0.488	....	1.74	SB
13974	200	−5.06	−0.38	−4.70	4.862	0.608	....	0.67	SB
16160	125	−5.75	−0.65	−4.96	5.821	0.972	13.03	....	...
17925	200	−4.12	−0.11	−4.29	6.043	0.867	....	−0.46	RS CVn
19373	0	−6.34	−1.00	−4.98	4.047	0.595	....	1.83	...
20630	210	−4.63	−0.36	−4.43	4.836	0.679	....	3.96	BY Dra
22049	150	−5.07	−0.44	−4.48	3.726	0.882	11.44	3.25	BY Dra
26690	275	−5.56	−0.60	....	5.289	0.364	....	0.99	SB
26965	0	−5.58	−0.14	−4.93	4.424	0.816	....	....	flare
27483	0	−5.07	−0.50	....	6.169	0.458	....	1.16	SB
28052[a]	100	−4.72	−0.05	....	4.492	0.249	....	0.36	δ Sct, SB
28294	130	−6.01	−0.66	....	5.895	0.327	....	0.23	...
32147	50	−5.88	−0.63	−4.94	6.230	1.052	....	....	SB
33564	0	−5.96	−1.00	−4.79	5.043	0.477	....	1.47	...
35296	257	−4.39	−0.12	−4.38	4.989	0.527	....	1.86	BY Dra
38393	100	....	....	−4.85	3.590	0.481	....	2.03	...
39587	275	−4.54	−0.27	−4.42	4.401	0.591	6.96	2.47	RS CVn
40136	100	−5.77	−0.36	....	3.713	0.332	....	0.67	....
43318	0	....	....	....	5.642	0.503	5.83	1.59	...
61421	0	−6.14	−0.90	−4.52	0.366	0.421	....	1.35	SB
64096	0	....	....	−4.82	5.169	0.596	11.38	1.61	SB
65626	230	−3.78	0.03	−4.48	6.490	0.620	....	−1.35	RS CVn
72905	175	−4.46	−0.32	−4.38	5.631	0.619	....	0.34	BY Dra
75732	50	−5.61	....	−5.04	5.946	0.862	13.13	....	...
76151	100	−5.25	−0.58	−4.69	6.001	0.663	11.56	1.40	...
78418	0	−5.42	−0.65	−4.93	5.956	0.665	11.57	0.60	SB
81809	0	−6.26	−0.89	−4.94	5.372	0.641	....	1.87	SB
82210[a]	200	−4.38	0.04	−4.50	4.568	0.769	11.22	1.31	RS CVn
85217	230	−4.77	−0.15	....	6.255	0.474	9.34	1.12	SB
88215	0	−6.22	−0.78	....	5.298	0.367	....	0.78	SB
88230	200	−4.32	−0.54	−4.51	6.597	1.372	....	....	flare
90839	0	−5.51	−0.67	−4.86	4.834	0.518	10.32	2.08	...
98230	295	−4.3	−0.21	....	4.830	0.620	....	....	SB
101501	100	−5.15	−0.75	−4.54	5.321	0.723	11.43	0.69	var
102870	0	−5.74	−0.63	−4.99	3.608	0.551	....	2.69	...
105452	0	−4.86	−0.33	....	4.021	0.332	....	0.53	...
110379	90	−5.11	−0.10	....	2.743	0.357	....	0.76	SB
112412	0	−5.47	−0.38	....	5.607	0.337	....	....	...
113337	0	−4.98	−0.04	−4.99	6.069	0.415	8.77	1.79	...
114378	200	−4.92	−0.38	−4.41	4.318	0.454	....	....	...
114710	50	−5.66	−0.72	−4.75	4.257	0.571	....	1.97	SB
115383	130	−4.41	−0.14	−4.40	5.209	0.585	10.21	2.21	...
116568	0	−5.16	−0.40	....	5.738	0.415	8.58	1.49	SB
121370	0	−6.50	−0.65	−5.25	2.681	0.580	....	2.79	SB
125451	0	−5.05	−0.13	−4.92	5.406	0.385	8.14	0.92	...
126660	133	−4.56	0.02	−4.33	4.052	0.497	....	1.78	var
128167	50	−5.55	−0.32	−5.07	4.465	0.364	....	0.69	var
129502	0	−5.23	0.16	....	3.879	0.383	....	0.94	...
131156	200	−4.44	−0.31	−4.35	4.562	0.768	10.85	....	BY Dra
137909	0	....	....	....	3.678	0.278	....	0.21	SB
141004	100	−6.21	−0.71	−4.95	4.427	0.603	11.52	2.72	SB
143761	50	−6.13	....	−5.03	5.417	0.601	11.62	1.77	...
144284	100	−5.04	−0.09	−4.47	4.004	0.524	....	2.24	SB
157214	50	....	....	−5.02	5.393	0.619	....	1.63	var
160922	0	−4.98	−0.28	−4.83	4.792	0.430	....	1.09	SB
161797	25	−6.23	−0.86	−5.11	3.418	0.751	....	2.91	...

Table 1. Continued.

HD	HeEW (mÅ)[b]	$\log(L_x/L_{bol})$	HR1[c]	$\log R'_{HK}$	V	$(B-V)$	$(m_{FUV}-B)$[d]	$c(19-27)$[e]	Notes[f]
165341	200	−4.93	−0.51	−4.55	4.022	0.863	....	1.95	BY Dra
170153	0	−6.16	−0.76	....	3.571	0.489	....	1.42	SB
173667	50	−5.27	−0.15	−4.86	4.202	0.455	....	1.56	var
201091	150	−5.46	−0.72	−4.64	4.840	1.260	....	....	BY Dra
201092	150	−5.50	....	−4.89	6.046	1.359	....	....	flare
210027	110	−5.76	−0.58	−4.36	3.769	0.433	....	1.05	SB
217014	0	....	....	−5.03	5.467	0.665	12.07	2.44	...

[a] One of the 100 X-ray-brightest stars within 50 pc of the Sun (Makarov 2003).
[b] Equivalent width of λ10830 He I triplet from Zarro & Zirin (1986).
[c] Soft X-ray hardness ratio from *ROSAT* data, e.g., Voges et al. (1999).
[d] (*GALEX* FUV magnitude) − (Johnson *B* magnitude).
[e] A colour from *TD-1* photometry in 2 740 and 1 965 Å bands.
[f] SB = spectroscopic binary; var = variable star.

Table 2. Data for additional dwarfs.

HD	HeEW (mÅ)[c]	Source[d]	$\log(L_x/L_{bol})$	HR1[e]	$\log R'_{HK}$	V	$(B-V)$	$(m_{FUV}-B)$[f]	$c(19-27)$[g]	Notes[h]
17433[b]	400	SD	− 3.2	−0.08	....	6.760	0.960	9.40	....	RS CVn
21242[b]	240	SD	− 3.3	−0.05	....	6.490	0.884	8.89	....	RS CVn
22049[a]	310	SD	− 5.07	−0.44	−4.48	3.726	0.882	11.44	3.25	BY Dra
98230[a]	380	SD	− 4.3	−0.21	....	4.830	0.620	....	....	SB
146361[b]	320	SD	− 3.4	0.06	−3.72	5.226	0.593	9.03	1.40	RS CVn
224085[b]	300	SD	− 2.8	−0.15	....	7.451	1.018	8.58	....	RS CVn
142373	45	TT	...	....	−5.07	4.622	0.559	....	1.50	...
165908	36	TT	− 6.10	....	−5.02	5.046	0.519	....	1.73	...
10700[a]	36	TT	− 6.21	−1.00	−4.97	3.495	0.727	....	....	...
131156[a]	291	TT	− 4.44	−0.31	−4.35	4.562	0.768	10.85	....	BY Dra
141004[a]	70	TT	− 6.21	−0.71	−4.95	4.427	0.603	11.52	2.72	...
196755	95	TT	− 5.82	−0.63	....	5.074	0.702	11.75	....	...
161797[a]	80	TT	− 6.23	−0.86	−5.11	3.418	0.751	....	2.91	...
182572	38	TT	− 6.25	....	−5.06	5.155	0.761	....	1.64	var

[a] Also included in Table 1.
[b] One of the 100 X-ray-brightest stars within 50 pc of the Sun (Makarov 2003).
[c] Equivalent width of λ10830 He I triplet.
[d] Source of He I EW: TT = Takeda & Takada-Hidai (2011); SD = Sanz-Forcada & Dupree (2008).
[e] Soft X-ray hardness ratio from *ROSAT* data (e.g., Voges et al. 1999).
[f] (*GALEX* FUV magnitude) − (Johnson *B* magnitude).
[g] A colour from *TD-1* photometry in 2 740 and 1 965 Å bands.
[h] SB = spectroscopic binary; var = variable star.

discussed in Section 4. In addition, some measurements of the C IV λ1549 emission line originating from the TR between corona and chromosphere are available in the literature, with Simon & Drake (1989) providing a homogeneous set of line strengths based on *IUE* spectra.

In an effort to obtain space-based photometric UV data for the stars in Tables 1–3, catalogues based on all-sky surveys made by the *TD-1* (Thompson et al. 1978) and *GALEX* (Martin et al. 2005; Morrissey et al. 2005; Bianchi 2014) spacecraft observatories were searched. Whilst the Belgian/UK Ultraviolet Sky Survey Telescope (Boksenberg et al. 1973) on board the *TD-1* satellite measured magnitudes through bandpasses extending to central wavelengths as short as 1 565 Å, the 1 965 Å bandpass is the shortest one for which reasonably useful data exist for the stars in Tables 1, 2, with few stars from Table 3 being represented. The *TD-1* data were used to form a colour $c(19–27) = -2.5\log(F1965/F2740)$, where $F2740$ and $F1965$ are fluxes in the 2 740 and 1 965 Å bands, respectively. This colour is listed in Tables 1–3, where it has been calculated from data in Thompson et al. (1978). Far-UV magnitudes were searched for within the *GALEX* DR6/7 releases (Bianchi 2014) for stars in Tables 1–3, and where available have been used to form a colour $(m_{FUV} - B)$ which is also tabulated. The bandwidth of the *GALEX* FUV band is 1 344–1 786 Å, with an effective wavelength of 1 528 Å (Morrissey et al. 2005).

3 THE He I TRIPLET VERSUS CORONAL SOFT X-RAY RELATIONSHIP

When Zarro & Zirin (1986) wrote their paper, the main database of coronal soft X-ray emission measurements of the stars in their programme came from the *Einstein* satellite.

Table 3. Data for metal-poor dwarf stars.

HD	HeEW (mÅ)[a]	Source[b]	log R'_{HK}	[Fe/H]	V	$(B-V)$	$(m_{FUV}-B)$[c]	$c(19-27)$[d]
19445	30	TT	....	−2.05	8.058	0.458	9.15	....
193901	41	TT	−4.97	−1.10	8.653	0.549	10.69	....
201891	26	TT	−4.86	−1.10	7.372	0.510	....	0.34
148816	30	TT	−4.92	−1.00	7.283	0.537	11.02	....
224930	33	TT	−4.92	−0.90	5.742	0.672	11.92	2.07
6582	37	TT	−4.96	−0.81	5.163	0.694	....	....
25329	67	SDS	−4.99	−1.75	8.501	0.866	....	....
31128	37	SDS	−4.88	−1.6	9.134	0.490	9.69	....
59374	38	SDS	....	−0.9	8.493	0.522	10.75	....
59984	22	SDS	−4.98	−0.7	5.902	0.540	....	1.13
64090	19	SDS	−4.92	−1.65	8.300	0.621	12.12	....
64606	14	SDS	−4.92	−0.9	7.435	0.733	....	....
74000	15	SDS	....	−2.1	9.667	0.419	7.84	....
76932	21	SDS	−4.72	−0.9	5.824	0.524	10.44	1.32
84937	27	SDS	....	−2.1	8.324	0.389	....	....
94028	35	SDS	....	−1.45	8.226	0.471	9.06	....
97916	40	SDS	....	−1.15	9.210	0.417	8.16	....
103095	56	SDS	−4.98	−1.35	6.445	0.751	....	....
188510	13	SDS	−4.91	−1.7	8.829	0.594	....	....
201889	37	SDS	−5.03	−1.0	8.058	0.589	....	....
221377	39	SDS	....	−0.95	7.570	0.390	8.35	....

[a]Equivalent width of λ10830 He I triplet.
[b]Source of He I EW: TT = Takeda & Takada-Hidai (2011); SDS = Smith, Dupree, & Strader (2012).
[c](*GALEX* FUV magnitude) − (Johnson *B* magnitude).
[d]A colour from *TD-1* photometry in 2 740 and 1 965 Å bands.

Since then the *ROSAT* All Sky Survey has been conducted (Voges et al. 1999). Where available for stars in the Zarro & Zirin (1986) sample, the soft X-ray luminosity L_x and Hardness Ratio HR1 as derived from *ROSAT* observations were obtained from Hünsch, Schmitt, & Voges (1998). The X-ray luminosities were converted to values of $\log(L_x/L_{bol})$ using the same *Hipparcos* distances adopted by Hünsch et al. (1998), together with V and $(B-V)$ from the GCPD, and the bolometric corrections of Flower (1996). In the case of seven stars, values of $\log(f_x/f_{opt})$ and HR1 were found in the *ROSAT* All-Sky Bright Source Catalogue (Voges et al. 1999; 1RXS), with the former again being transformed to $\log(L_x/L_{bol})$ using the GCPD photometry and Flower (1996) bolometric corrections. The particular *ROSAT* Hardness Ratio compiled in Table 1 is HR1 = (H−S)/(H+S) (Neuhaeuser et al. 1995; Voges et al. 1999), where S refers to the count rate in the 0.1–0.4 keV channel and H to the count rate in an energy band of 0.5–2.0 keV. The parameter HR1 depends upon the coronal plasma temperature and absorbing neutral hydrogen column density along the line of sight to a source, e.g., Neuhaeuser et al. (1995). Measurements of $\log(L_x/L_{bol})$ for the stars HD 75732, HD 143761, HD 201092, and HD 217014, were obtained from Katsova & Livshits (2011), whilst a value of −4.3 from Sanz-Forcada & Dupree (2008) is used for HD 98230.

The correlation between the *Einstein*-based measurements of $\log(L_x/L_{bol})$ used by Zarro & Zirin (1986) and the *ROSAT* measurements compiled here is shown in Figure 1. The data scatter about the 1:1 relation corresponding to equality between the two luminosity scales, which is shown as a solid line. The mean value of the difference between *ROSAT* and the *Einstein* measurements from Zarro & Zirin

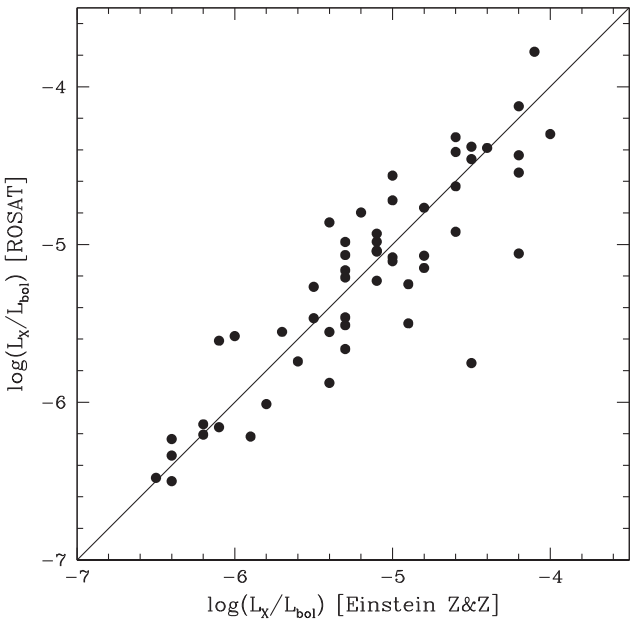

Figure 1. Soft X-ray luminosities $\log(L_x/L_{bol})$ of dwarf stars in the Zarro & Zirin (1986; ZZ) programme as measured by the *ROSAT* satellite versus the earlier values employed by ZZ as measured by the *Einstein* satellite. The solid line is the relation for equality between the plotted parameters.

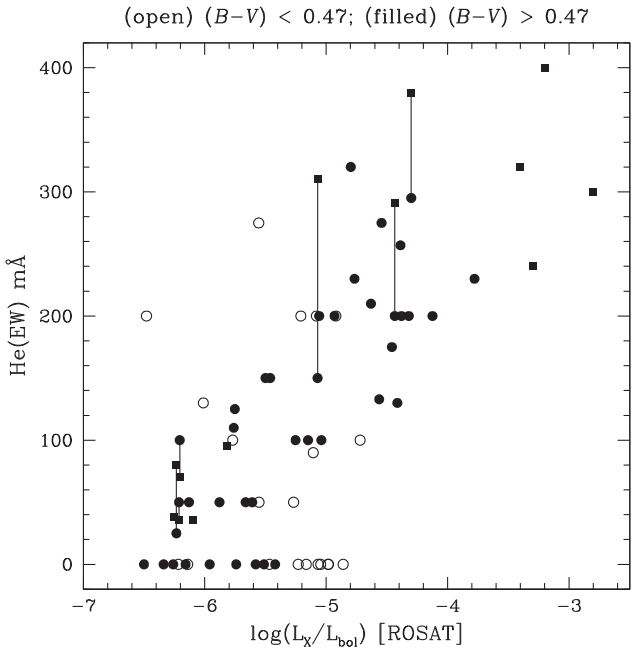

Figure 2. The equivalent width of the λ10830 He I feature versus soft X-ray luminosity $\log(L_x/L_{bol})$ as measured by the *ROSAT* satellite for dwarf stars in Tables 1 and 2. Data from the Zarro & Zirin (1986) programme as compiled in Table 1 are plotted with filled or open symbols according to whether stars are redder or bluer than $(B-V) = 0.47$, respectively. Filled boxes depict data from Table 2 (all stars from which have $B-V > 0.47$). Vertical lines connect data points for those six stars that appear in both tables.

is $\Delta \log(L_x/L_{bol}) = -0.04$, with a standard deviation of 0.33.

The sample of Population I dwarfs from Zarro & Zirin (1986) has been expanded through inclusion of He λ10830 EW and L_x data given in Sanz-Forcada & Dupree (2008) and Takeda & Takada-Hidai (2011). There are six stars in common between these two works and Zarro & Zirin (1986), for which the (L_x/L_{bol}) data from Table 1 are repeated in Table 2, whilst for the other stars in Table 2, the values of (L_x/L_{bol}) are from SD and TT, being also derived from *ROSAT* observations. Values of the Hardness Ratio HR1 as obtained from Voges et al. (1999) are also included in Table 2.

Figure 2 is a plot of the He I λ10830 EW against the coronal soft X-ray emission as measured by *ROSAT*. This figure updates the main result of Zarro & Zirin (1986), and it includes stars from both Tables 1 (circles) and 2 (boxes). Coronal soft X-ray emission is subject to saturation at high levels of $(L_x/L_{bol}) \sim 10^{-3.1}$ (Pizzolato et al. 2003; Wright et al. 2011, 2013; Gondoin 2013), and several of the dwarfs in Table 2 approach this limit, whilst the highest values amongst the Zarro & Zirin (1986) stars are $(L_x/L_{bol}) \sim 10^{-4}$. Thus, the dwarf stars in Figure 2 encompass close to the full intrinsic range in normalised soft X-ray emission. Several of the stars in Tables 1 and 2 are included in a list of the 100 brightest X-ray stars within 50 pc of the Sun compiled by Makarov (2003).

The dwarfs from Table 1 are depicted in Figure 2 according to their $B-V$ colour, as either open circles ($B-V < 0.47$) or filled circles ($B-V > 0.47$). Such a distinction based on $(B-V)$ follows Zarro & Zirin (1986), who found a correlation between He I λ10830 strength and L_x/L_{bol} for the cooler (later than F7V), but not the hottest, dwarfs in their sample. A slightly different value of $(B-V)$ is used here at which to divide the stars in Table 1, but the conclusions of Zarro & Zirin (1986) still stand with the use of the *ROSAT* data. Included in Figure 2 are stars from Table 2, which are represented by filled boxes, and all of which have optical colours of $(B-V) > 0.47$. Vertical lines connect data points for those six stars that appear in both Tables 1 and 2.

There is no obvious correlation between λ10830 EW and $\log(L_x/L_{bol})$ amongst the dwarfs with $(B-V) < 0.47$. The lack of correlation amongst the earlier F dwarfs is consistent with the findings of Smith (1983), as well as Zarro & Zirin (1986). However, amongst those dwarfs from Table 1 with $(B-V) > 0.47$, there is a Pearson correlation coefficient of 0.81 between the λ10830 EWs from ZZ and values of L_x/L_{bol} from *ROSAT*. If the stars from Table 2 are added to the sample, with equal weights being given to the EW measurements in Tables 1 and 2 for stars in common, the Pearson correlation coefficient is little changed, being increased slightly to $r = 0.83$, indicative of a strong correlation between He Iλ10830 triplet strength and soft X-ray luminosity amongst dwarfs with $(B-V) > 0.47$.[1] Residuals in He I EW about a least-squares fit to the data in Figure 2 for $(B-V) > 0.47$ show no correlation with $B-V$ colour.

Pearson coefficients were also calculated for samples from Tables 1 and 2 with several other lower limits in $(B-V)$ colour. Using data from these tables for stars restricted to $(B-V) > 0.52$ gives a correlation coefficient of $r = 0.84$, which is little different from what is obtained when taking a $(B-V)$ limit of 0.47 mag. A similar result is found when data are taken only from Table 1 for this colour limit. By contrast, if the sample from Table 1 alone is used but expanded to include data points for all stars with $(B-V) > 0.42$, then the value of r decreases to 0.76. Therefore, the inclusion of dwarfs marginally bluer than a limit of $(B-V) = 0.47$ weakens somewhat the correlation between λ10830 EW and soft X-ray luminosity. Considering all data from Table 1 increases the sample to 61 stars but decreases the correlation coefficient to $r = 0.57$. As such, the data suggest that a correlation does not exist between λ10830 EW and soft X-ray luminosity for early F dwarfs, as discussed originally by Zarro & Zirin (1986).

Whether there is a well-defined effective temperature boundary between dwarfs which do and do not follow a EW-(L_x/L_{bol}) correlation probably cannot be answered until a larger set of λ10830 data becomes available, say for several hundred dwarfs having a range not only in $(B-V)$ but also

[1] This is a slightly stronger correlation than found by Sanz-Forcada & Dupree (2008) for dwarfs and subgiants, who also incorporated data from Zarro & Zirin (1986) in their (Figure 9) plot of L_x/L_{bol} versus λ10830 EW.

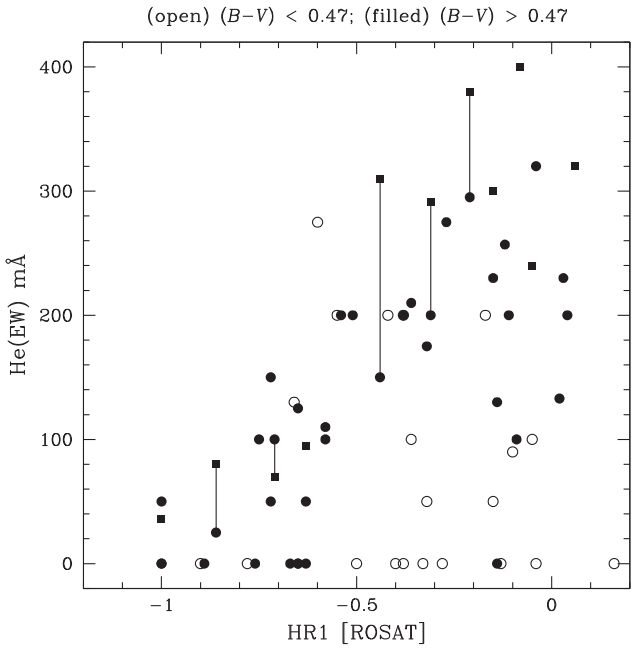

Figure 3. The equivalent width of the λ10830 He I feature versus Hardness Ratio HR1 of the soft X-ray spectrum as measured by *ROSAT* for stars in Tables 1 and 2. The symbols are chosen on the basis of the $(B-V)$ colour of each star: open circles ($B-V<0.47$), filled circles, and filled boxes ($B-V>0.47$). Vertical lines connect data points for stars that appear in both tables.

metallicity. A $(B-V)$ colour of 0.47 with a solar metallicity corresponds to an effective temperature for a dwarf star of $T_{\rm eff}=6\,360$ K according to the calibration defined by equations (1) and (2) plus Tables 2 and 4 of Ramírez & Meléndez (2005). By contrast, a more metal-poor dwarf with [Fe/H] $=-1.0$ and the same $(B-V)$ has an effective temperature of 6 025 K. Consequently, if there is a unique upper limit in $T_{\rm eff}$ to dwarfs that satisfy a EW-$(L_{\rm x}/L_{\rm bol})$ correlation, a range in [Fe/H] within a sample of such stars will smear out the $(B-V)$ colour of that boundary.

The He I EW is plotted against the *ROSAT* hardness ratio HR1 in Figure 3 for the dwarfs from Tables 1 and 2. Symbols in this figure follow the same convention as in Figure 2, namely filled circles for stars from Table 1 with $(B-V)>0.47$, open circles for stars from Table 1 with $B-V$ less than this, and filled boxes for dwarfs from Table 2 (all of which are redder than $B-V=0.47$). There is no correlation, but what does seem indicated is that high EWs of more than 160 mÅ tend to be mainly found amongst dwarfs with HR1 >-0.60. The median value of the *ROSAT* HR1 ratio for late-type dwarfs is ~-0.25 (Meurs, Casey, & Norci 2003, 2006). Thus, many of the dwarfs with strong He I λ10830 have values of HR1 that are otherwise typical of late-type dwarfs. By contrast, 95% of the most X-ray-luminous dwarfs within 50 pc of the Sun have HR1 >-0.20 and a narrow distribution which peaks near HR1 ~ 0.0 (Makarov 2003).

Amongst dwarfs with $(B-V)>0.47$, the distribution of HR1 values in Figure 3 is different between those stars with a He I triplet weaker than 160 mÅ, for which the average value of HR1 is -0.62 (with a standard deviation of $\sigma=0.29$), and stars with stronger λ10830 lines, for which the mean HR1 is -0.21 ($\sigma=0.19$). Thus, the X-ray spectra of the strong-triplet-line dwarfs of late-F, G, and K spectral types are more weighted towards harder energy distributions than those of weak-triplet dwarfs of the same range of spectral type. Perhaps also worth noting is that amongst the weaker triplet stars with EW ≤ 100 mÅ, the early-F dwarfs with $(B-V)<0.47$ have a harder X-ray spectrum, on average, than the later F dwarfs.

The lack of a correlation in Figure 3 for later-type dwarfs with $(B-V)>0.47$ is due in part to four stars from Table 1 with λ10830 EW$\leq$140 mÅ that nonetheless have HR1 hardness ratios greater than -0.2. These four stars are HD 26965, HD 115383, HD 126660, and HD 144284. The first is a dwarf that is known to have flare activity, the third star is a variable, whilst the fourth is a spectroscopic binary (SB). Interpretation of the positions of these stars in Figure 3 might hinge on whether there is any time variability in their triplet lines or X-ray spectra.

An HR1 value greater than -0.5 does not guarantee a strong λ10830 triplet line, but might it be a necessary condition for such? In the plasma models of Neuhaeuser et al. (1995) and Carr, Meurs, & Cunniffe (2004), the value of HR1 is very sensitive to the column density of any absorbing hydrogen in the line of sight. There is no correlation between either He I EW or HR1 and distance from the Sun for the stars in Tables 1 and 2, and they are sufficiently close that interstellar absorption may be of little import on HR1 (Kastner et al. 2003). Thus, variations in H I column density between stars may not be the reason for the range of HR1 in Figure 3. Dwarfs with large He I triplet strengths that exceed $\sim$ 150 mÅ may have hotter coronae than some, but by no means all, lower activity dwarfs.

Two Hardness Ratios are often given from *ROSAT* data. In addition to HR1, there is HR2 (Neuhaeuser et al. 1995) which defines the slope of the spectrum within the 0.4–2.0 keV energy range. For stars in Tables 1 and 2, values of HR2 were obtained where available from Voges et al. (1999). A resulting plot of HR2 versus HR1 for dwarfs unrestricted in $(B-V)$ colour is shown in Figure 4. In this diagram, the filled and open triangles denote dwarfs with He I λ10830 EW of >120 and <120 mÅ, respectively. The stars in Figure 4 occupy a region of this diagram that is also populated by Hyades cluster dwarfs and nearby field dwarfs within 14 pc of the Sun (Kastner et al. 2003). A Pearson cross-correlation coefficient for the data in Figure 4 is $r=0.68$, indicative of a modest correlation between the two Hardness Ratios, and a least-squares fit is shown in the figure as a solid line. The mean value of HR1 for stars in Figure 4 is -0.33, close to the value found by Meurs, Casey, & Norci (2006) for late-type dwarfs, with a standard deviation of $\sigma=0.26$. The comparable mean and σ for HR2 are -0.17 and 0.24, respectively. There is no

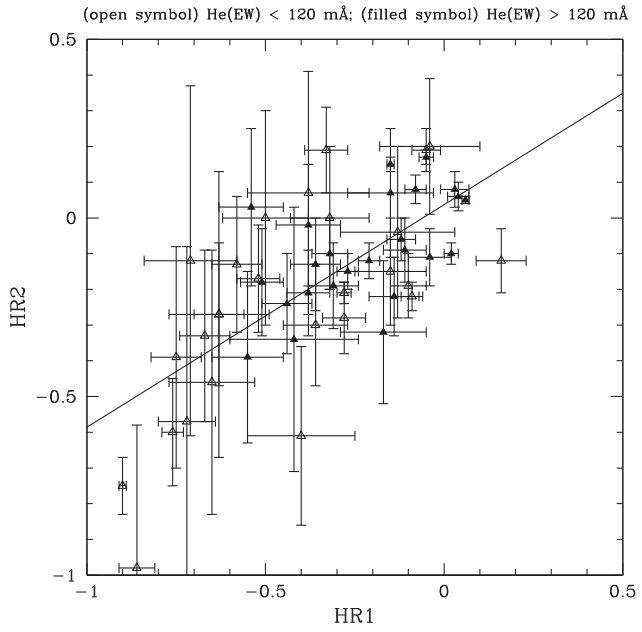

Figure 4. The Hardness Ratios HR2 versus HR1 of the soft X-ray spectrum as measured by *ROSAT* for dwarfs in Tables 1 and 2. The symbols are chosen on the basis of the equivalent width of the He I λ10830 triplet feature: (filled triangles) EW >120 mÅ; (open triangles) EW <120 mÅ. The solid line shows a least-squares fit of HR2 versus HR1.

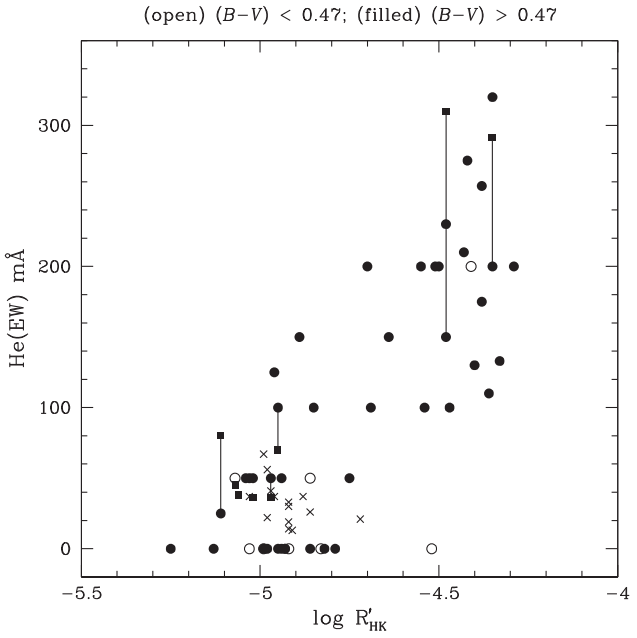

Figure 5. Equivalent width of the λ10830 He I feature versus the chromospheric Ca II emission index $\log R'_{\rm HK}$ for Population I dwarfs in Table 1 (circles), Table 2 (filled boxes), and metal-poor subdwarfs of Population II from Table 3 (crosses). Vertical lines connect data points for stars with $R'_{\rm HK}$ indices that appear in both Tables 1 and 2.

indication of an offset in Figure 4 between those weak-triplet and strong-triplet dwarfs for which HR1 > -0.6, however, both Figures 3 and 4 indicate that dwarfs with HR1 < -0.6 have He I λ10830 lines weaker than 160 mÅ. Some weak-He-triplet dwarfs may extend to softer X-ray spectra than dwarfs with a triplet EW in exess of 160 mÅ, but there are a number of dwarfs which have comparable pairs of (HR1, HR2) regardless of the λ10830 line strength.

A model grid of HR1 versus HR2 was calculated by Neuhaeuser et al. (1995) for single-temperature Raymond & Smith (1977) spectra and a range in absorbing hydrogen column density of $\log(N_H/{\rm cm}^{-2}) = 18$–$21$. The data in Figure 4 predominantly fall outside of the Neuhaeuser et al. (1995) grid in the sense of requiring lower N_H than 10^{18} cm^{-2}. By contrast, thermal Bremmstrahlung models computed by Carr et al. (2004) for $N_H \sim 0.5 - 2 \times 10^{20}$ cm^{-2} are more successful in matching the datapoints of Figure 4.[2]

4 THE He I TRIPLET VERSUS CHROMOSPHERIC Ca II H AND K EMISSION

Vaughan & Zirin (1968) concluded from Palomar 200-in coudé spectra of G and K stars that 'there is a rough statistical tendency for λ10830 absorption to increase in strength with increasing Ca II K emission intensity'. Since the start of the Mount Wilson HK project (Vaughan, Preston, & Wilson 1978; Vaughan & Preston 1980), there has been a great expansion in the amount of quantitative data on the chromospheric Ca II H and K emission lines of late-type dwarfs.

Quite a few of the Zarro & Zirin (1986) stars are included in a compilation of $\log R'_{\rm HK}$ values assembled by the present author. The properties of this compilation are described in Smith & Redenbaugh (2010) and Smith, Redenbaugh, & Jones (2011) who give a discussion of the various data sets from the literature that were used. The main sources on which the compilation is based are Noyes et al. (1984), Soderblom (1985), Soderblom, Duncan, & Johnson (1991), Henry et al. (1996), Gray et al. (2003, 2006), Wright et al. (2004), and Jenkins et al. (2006, 2008). Values of $\log R'_{\rm HK}$ from these sources, homogenised as described in Smith et al. (2011), are included in Tables 1–3. In addition, $R'_{\rm HK}$ data are included for some stars in Tables 1–3 from the following references: Baliunas, Sokoloff, & Soon (1996a), Isaacson & Fischer (2010), Katsova & Livshits (2011), Pace (2013), Santos et al. (2011), Schroeder, Reiners, & Schmitt (2009), and Vican (2012).

Figure 5 shows the He I λ10830 EW plotted versus $\log R'_{\rm HK}$ for the dwarf stars from Zarro & Zirin (Table 1), with filled and open circles again denoting dwarfs redder and bluer than $(B-V) = 0.47$, respectively. Stars from Table 2 are represented as filled boxes, and vertical lines connect data points for stars that appear in both Tables 1 and 2. There is a correlation between the λ10830 EW and strength of the Ca II H+K emission. Weighting data points from Tables 1 and 2 equally, the Pearson correlation coefficient between λ10830 EW and $\log R'_{\rm HK}$ is $r = 0.83$, so that the correlation is of comparable

[2] An interstellar reddening of $E(B-V) = 0.01$ mag in the vicinity of the Sun corresponds to a column density of $N_H \sim 5 \times 10^{19}$ cm^{-2} according to equation (4) of Neuhaeuser et al. (1995).

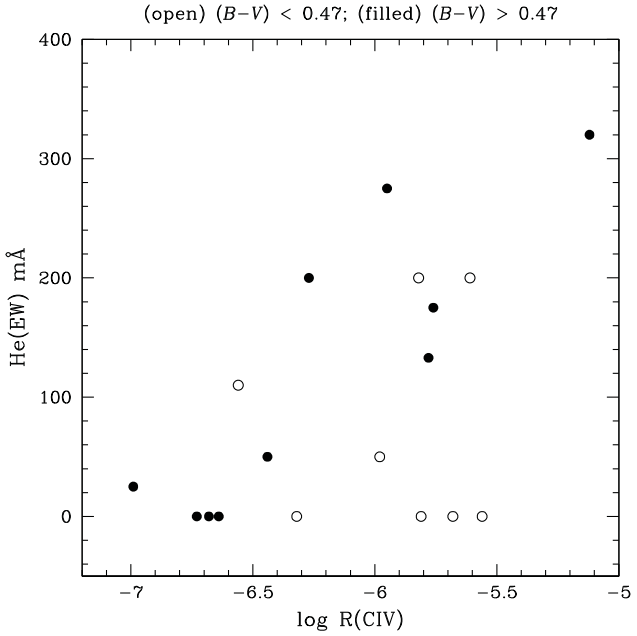

Figure 6. The equivalent width of the λ10830 He I feature versus the luminosity in the transition region λ1549 emission line of C IV, as normalised to bolometric luminosity. The symbols are again based on stellar colour: open circles ($B-V$ < 0.47), filled circles ($B-V$ > 0.47).

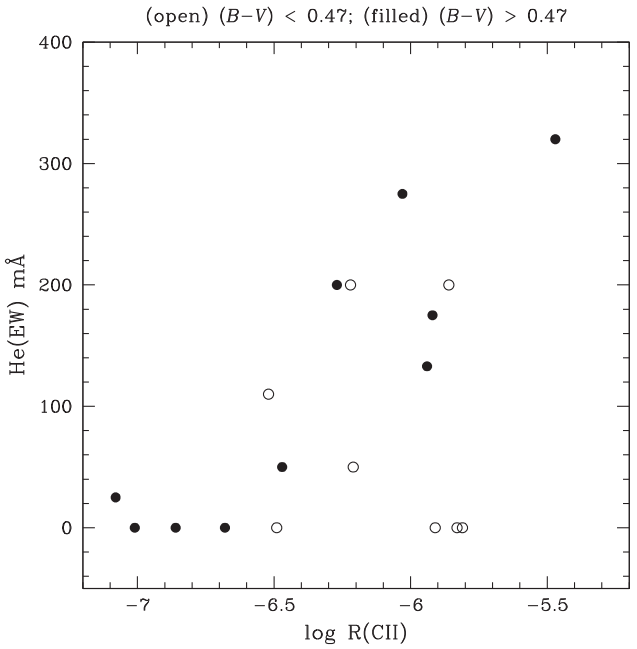

Figure 7. The equivalent width of the λ10830 He I triplet versus the ratio of luminosity in the λ1335 emission line of C II normalised to bolometric luminosity. The symbols are based on stellar colour: open circles ($B-V$ < 0.47), filled circles ($B-V$ > 0.47).

significance to that between λ10830 EW and soft X-ray luminosity. Nonetheless, there is a substantial scatter in triplet EW of ∼ 200 mÅ amongst the dwarfs with the strongest H and K emission. Some of this scatter is likely the result of observational uncertainty, but it may also be partly a product of intrinsic variability.

Two of the Population I dwarfs in Table 1 with the lowest R'_{HK} are HD 121370 and HD 161797, which are classified as spectral type G0IV and G5IV, respectively. As such, both stars have evolved somewhat away from the zero age main sequence (ZAMS) and may be an example of the phenomenon pointed out by Wright (2004), who found that a large fraction of so-called 'Maunder-Minimum' dwarfs have evolved a magnitude or more brighter than the ZAMS. Furthermore, HD 121370 is a spectroscopic binary (SB), and the R'_{HK} index may be affected by light from the spectroscopic companion.

5 RELATIONS WITH C IV λ1549 AND C II λ1335 EMISSION

A number of the stars in the Zarro & Zirin (1986) list of Table 1 are included in a survey of λ1335 C II and λ1549 C IV emission line strengths by Simon & Drake (1989). The C IV emission line arises from a TR between the corona and chromosphere, and so is a complement to both coronal soft X-ray and chromospheric Ca II emission. Stars in common between Zarro & Zirin (1986) and Simon & Drake (1989) are shown in Figure 6, wherein the λ10830 He I EW is plotted against R(C IV), which is the luminosity of the C IV line normalised to stellar bolometric luminosity. The symbol convention is based on $B-V$ colour as in several previous figures.

The pattern in Figure 6 is rather reminiscent of that in Figure 2, with a correlation between He λ10830 EW and C IV luminosity being evinced by dwarfs cooler than $(B-V) = 0.47$, but not by hotter dwarfs. Thus, in accord with various correlations present between coronal, TR, and chromospheric emission from G and K dwarfs (e.g., Ayres, Marstad, & Linsky 1981; Simon & Drake 1989), the soft X-ray emission is not the only stellar activity indicator with which He I triplet absorption correlates.

The relationship between the He I and C IV lines for some high-activity dwarfs in Table 2 has been discussed by Sanz-Forcada & Dupree (2008). Their Figure 10 shows no clear correlation for dwarfs with λ10830 EW greater than 150 mÅ, on the basis of which they argued that at very high levels of activity amongst dwarf stars, the He I λ10830 line saturates and becomes decoupled from high-energy photons emitted by the corona. Nonetheless, in a comparison between dwarfs with low to mid-levels of activity, a correlation can be discerned for dwarfs of $(B-V) > 0.47$, with the Pearson correlation coefficient for the 10 such dwarfs in Figure 6 being $r = 0.87$.

A corresponding plot of He I λ10830 EW versus λ1335 C II luminosity is presented in Figure 7, and shows much the same characteristics as Figure 6, with a correlation being present amongst dwarfs cooler than $(B-V) > 0.47$, but not amongst hotter F dwarfs.

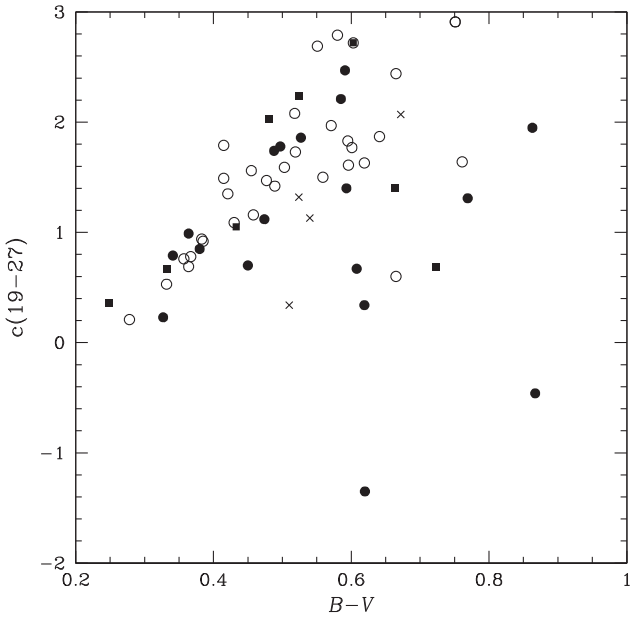

Figure 8. The $c(19–27)$ colour from *TD-1* photometry versus $(B-V)$ for dwarf stars. In the case of stars from Tables 1 and 2, the symbols denote the equivalent width of the He I λ10830 feature: (open circles) EW < 100 mÅ; (filled boxes) EW = 100–110 mÅ; (filled circles) EW > 110 mÅ. Metal-poor subdwarfs from Table 3 are represented by crosses.

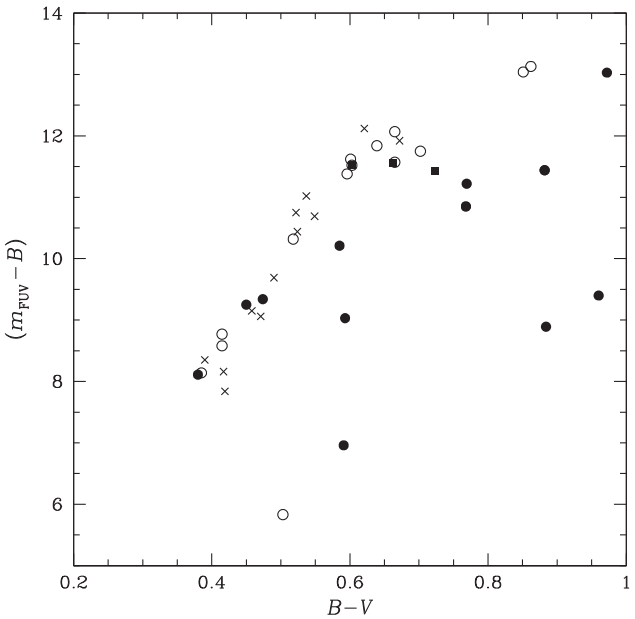

Figure 9. A *GALEX*-derived colour $(m_{\rm FUV}-B)$ versus $(B-V)$ for dwarfs in Tables 1–3. Symbols follow the same system as for Figure 8: (open circles) stars with He I EW < 100 mÅ from Tables 1 and 2; (filled boxes) stars with He I EW of 100–110 mÅ from Tables 1 and 2; (filled circles) stars with EW > 110 mÅ from Tables 1 and 2; (crosses) metal-poor subdwarfs from Table 3.

6 He I TRIPLET VERSUS UV FLUX RELATIONS

The $c(19-27)$ colour derived from *TD-1* data is plotted versus $(B-V)$ in Figure 8, where the point types used for dwarfs from Tables 1 and 2 are set by the EW of the He I λ10830 triplet (open circles for EW less than 100 mÅ; filled boxes for EW = 100–110 mÅ; filled circles for EW ≥ 110 mÅ). Amongst Population I dwarfs with $(B-V)<0.60$, there is little distinction on the basis of He I EW between points in Figure 8. However, for Population I dwarfs with redder $(B-V)$ colours, stars with the strongest He I lines tend to have bluer *TD-1* colours, with $c(19-27)<1.5$, than low-activity dwarfs, although there are a couple of exceptions.[3] Thus, the cooler dwarfs may be exhibiting a dependence of $c(19–27)$ on stellar activity.

Four metal-poor subdwarfs from Table 3 are plotted in Figure 8 as crosses. The metal-poor subdwarfs tend to be displaced towards bluer $c(19–27)$ colours relative to many low-activity Population I dwarfs of comparable $(B-V)$ colour. This could be a result of much weaker metal-line blanketing of the ultraviolet spectrum of the Population II subwarfs. However, there is sufficient scatter amongst the Population I dwarfs in Figure 8 as to make this inference a rather weak one.

The *GALEX*-based $(m_{\rm FUV}-B)$ colour is plotted against $(B-V)$ in Figure 9 for stars in Tables 1–3. Symbols are chosen according to He I λ10830 EW according to the convention of Figure 8. Metal-poor subwarfs from Table 3 follow much the same locus as the low-activity Population I dwarfs from Tables 1 and 2, with a λ10830 EW less than 100 mÅ. There is no offset between low-activity Population I and Population II stars in Figure 9. Amongst dwarfs with $(B-V)<0.55$ those with a strong He I λ10830 line follow a similar locus in Figure 9 to low-activity stars. However, the later spectral-type dwarfs in Figure 9 with λ10830 EW > 110 mÅ do show striking offsets in $(m_{\rm FUV}-B)$ from the low-activity dwarfs. This is consistent with the findings of Smith & Redenbaugh (2010) and Findheisen, Hillenbrand, & Soderblom (2011) that the *GALEX* FUV bandpass is sensitive to activity in the chromosphere and TR of dwarf stars.

The *GALEX* FUV band contains TR emission lines such as λ1393 Si IV and λ1549 C IV. Furthermore, Linsky et al. (2012) demonstrated that continuum emission in the FUV 1 150–1 500 Å region is sensitive to the level of stellar activity. They found that the continuum flux in this wavelength range correlates with rotation period and hence dynamo activity amongst solar-type stars. Their results also show a correlation between FUV continuum flux and that of the Si IV λ1393 line. There is a level of continuum flux in the 1 600–2 000 Å region that comes from the chromosphere and is sensitive to conditions near the temperature minimum between the photosphere and chromosphere (Haisch & Basri 1985). Indeed, the FUV continuum flux has been used as a constraint on models of the temperature structure of solar and stellar chromospheres (Vernazza, Avrett, & Loesser 1976,

[3] One star in Figure 8 (HD 141004) is plotted with both a box and an open circle because of a 30 mÅ difference in two EW measurements listed in Tables 1 and 2. Such a difference could be accounted for by uncertainties in the He I EW data.

1981; Morossi et al. 2003). Thus, the separation of G and K dwarfs in Figure 9 according to He I λ10830 EW could result from both TR line emission and chromospheric continuum emission in the *GALEX* FUV bandpass, and thereby has the same ultimate origin as the correlations seen in Figures 5–7.

7 THE He I TRIPLET AMONGST METAL-POOR SUBDWARFS

Measurements of the λ10830 He I EW of subdwarfs with low Population II metallicities have become available from Takeda & Takada-Hidai (2011) and Smith et al. (2012). These are compiled in Table 3 along with other ancillary data. There are very few soft X-ray detections by *Einstein* or *ROSAT* of these stars, and Smith, Dupree, & Günther (2016) report non-detections of three of these stars in deep exposures made by the *XMM-Newton* spacecraft observatory. Nonetheless, measurements of the chromospheric index $\log R'_{\rm HK}$ have been gleaned from the literature for some of the stars in Table 3.

Points for metal-poor subdwarfs are included as crosses in the Figure 5 plot of He triplet EW versus $\log R'_{\rm HK}$, wherein they fall near the lower left (low-activity) corner of the diagram. These subwarfs have weak Ca II H and K emission consistent with old ages, weak dynamos, and inactive chromospheres.

The metal-poor subdwarf with the strongest He I line is HD 25329. There is nothing remarkable about this star as judged from the data assembled for it in SIMBAD, and it is not listed as a member of either a spectroscopic or visual binary. HD 25329 is the coolest subdwarf in Table 3, and perhaps has a chromosphere like that of HD 103095, which is another cool subwarf in Table 3 having only a slightly weaker He I λ10830 line. Coincidentally, HD 103095 was found by Beardsley, Gatewood, & Kamper (1974) to be a possible flare star.

Population II subdwarfs in Figure 5 have values of $\log R'_{\rm HK}$ that are no lower than those of the least active Population I dwarfs from Tables 1–2. There are at least two complicating factors to hinder interpretation of this comparison, the first being the post-ZAMS evolution of some Population I dwarfs, as noted in the preceding section, whilst a second is the effect of metallicity on the photospheric contribution to $\log R'_{\rm HK}$, which can be significant in the comparison bandpasses used to measure this index (Soon et al. 1993; Rocha-Pinto & Maciel 1998; Hall et al. 2009).

8 SOME CONTEXT FOR THE STARS IN TABLES 1–3

The stars included in the primary He I EW data source used here from Zarro & Zirin (1986) are of a heterogeneous nature. Context for some stars, as obtained from SIMBAD (Wenger et al. 2000), is given in the Notes column of Tables 1 and 2. There are stars from the RS CVn and BY Dra high-activity categories, as well as a few flare stars, numerous SBs, and several other categories of variable stars (var). Additional context for the stars in the Zarro & Zirin survey comes from

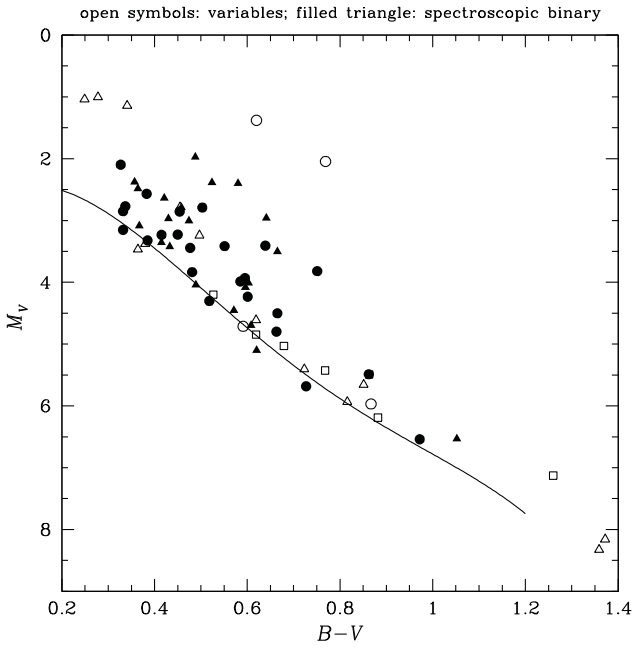

Figure 10. The M_V versus $(B-V)$ colour–magnitude diagram for the dwarf stars in the Zarro & Zirin (1986) survey (Table 1). Open circles depict RS CVn stars; open boxes correspond to BY Dra variables; other types of variable stars and flare stars are indicated by open triangles; spectroscopic binaries are shown with filled triangles; and all other stars are assigned filled circles. The solid line shows the ZAMS from VandenBerg & Poll (1989).

a colour–magnitude diagram shown in Figure 10. Absolute magnitudes M_V in this figure are based on the V magnitudes from Table 1 and the parallaxes on the *Hipparcos* system described by van Leeuwen (2007), as obtained from SIMBAD. A solid line in Figure 10 shows the ZAMS locus of VandenBerg & Poll (1989). This ZAMS relation constitutes a fiducial locus relative to which a difference in absolute magnitude was determined for the dwarfs in Table 1, a residual being calculated at the relevant value of $(B-V)$ for each star. A plot of the He I line strength versus the absolute magnitude residual $\Delta M_V = M_V - M_{V,\rm ZAMS}$ for the stars in Table 1 is presented in Figure 11. In both Figures 10 and 11, a convention is used whereby different types of stars are denoted with different symbols. Open symbols depict various types of variable or binary stars: RS CVn stars (open circles), BY Dra binaries (open boxes), and open trangles for other types of variables. SBs are shown by filled triangles. All other types of star are shown as filled circles.

Strong He I lines are found amongst both the RS CVn binaries and BY Dra stars of Tables 1 and 2, which are otherwise known for their high levels of stellar activity (e.g., Strassmeier et al. 1988; Eker 1992; Dempsey et al. 1993; Fernández-Figueroa et al. 1994, Makarov 2003). The former of these systems involve a main sequence or subgiant companion to a G or K giant or subgiant (Hall 1976), whereas the later are typically binary systems with main-sequence components (Bopp & Fekel 1977). Of the four RS CVn systems in Figures 10 and 11 (open circles), two fall close to the ZAMS

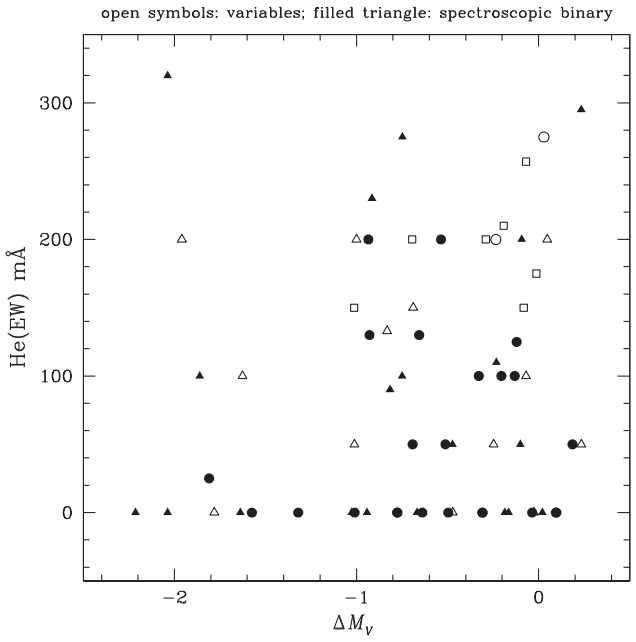

Figure 11. He I λ10830 equivalent width versus an absolute magnitude residual ΔM_V measured relative to the ZAMS for stars in Table 1. Open circles depict RS CVn stars; open boxes correspond to BY Dra variables; other types of variable stars and flare stars are indicated by open triangles; spectroscopic binaries are shown with filled triangles; and all other stars are assigned filled circles.

and the other two more than 3 mag above, but all four have strong He I lines. BY Dra stars (open boxes in Figures 10 and 11) have He I EWs in excess of 120 mÅ. Also, commonly seen to have He I EWs greater than 50 mÅ are dwarfs classified either as a flare star or other type of variable (open triangles in Figures 10 and 11) in the SIMBAD data repository. Given the role that RS CVn and BY Dra binaries play in constituting the most active objects in the Zarro & Zirin (1986) survey, benefit could be had from observing the He I λ10830 line amongst a larger sample of such stars, particularly with regard to documenting the degree to which the triplet absorption is variable with time at the highest levels of stellar activity.

HD 22049 is one star observed by Zarro & Zirin (1986) for which a higher resolution spectrum was obtained by Sanz-Forcada & Dupree (2008), who found a notably higher λ10830 EW of 310 mÅ (Table 2). Since HD 22049 is a BY Dra variable, the difference between the two EW measurements may be at least in part the result of time variability. The vertical line connecting the two points for this star in Figure 2 offers an illustration of the degree to which variability amongst highly active stars could impose scatter on correlations between He I λ10830 EW and other corona/TR/chromospheric proxies. Osten & Brown (1999) and Sanz-Forcada, Brickhouse, & Dupree (2002) found that RS CVn stars show pronounced EUV variability, in some cases linked to large flares. Thus, one would expect marked λ10830 variability for this category of active stars as well.

Amongst stars in the Zarro & Zirin (1986) sample that are more than 1.2 mag brighter in M_V than the ZAMS, it is only amongst the RS CVn binaries, SBs, or known variable stars that the He I EW exceeds 50 mÅ. Several of the dwarfs in the lower left corner of Figure 11, with $\Delta M_V < -1.2$, have embarked upon their evolution away from the main sequence. Their relatively weak λ10830 absorption is consistent with the trend found by Wright (2004) for chromospheres to approach Maunder-minimum levels of activity upon stellar evolution up to several magnitudes away from the ZAMS.

9 DISCUSSION

Zarro & Zirin (1986) used the correlation between soft X-ray luminosity and He I λ10830 EW amongst late-F, G, and K dwarfs, to support the theory that EUV photons from the corona were exciting the lower level of the He I triplet via the EUV-PR mechanism. However, it has been shown in this paper that the λ10830 EW also correlates with parameters that are directly set by conditions in the lower chromosphere, such as Ca II H and K emission, and to some extent the FUV flux in the 1 000–2 000 Å range. Given the correlations that exist between soft X-ray luminosity and various other chromospheric and TR indicators (e.g., Ayres et al. 1981; Jordan et al. 1987), it would seem that whilst the correlations presented above verify a link between the He I triplet and stellar activity in a general sense, none of the correlations can provide an unambiguous proof of a connection between He I EW and the strength of the EUV flux from a cool dwarf (see also O'Brien & Lambert 1986 for the case of λ10830 formation in the chromospheres of giant stars).

It was for this reason that Sanz-Forcada & Dupree (2008) measured He I λ10830 EWs for a sample of high-activity stars that were chosen to have EUV flux data from the *EUVE* satellite. They found no correlation between λ10830 EW and EUV luminosity for high-activity dwarfs, although their sample is small, leading them to conclude that for such stars collisional population of the lower state of the He I λ10830 transition is more significant than recombination following EUV-photon-induced ionisation. Lanzafame & Byrne (1995) found that collisional processes can dominate the formation of He I λ10830 for active late-type dwarfs such as ϵ Eri (HD 22049), which is one of the enhanced-triplet stars in Table 1 with an EW of 150 mÅ. Their models for ϵ Eri can predict an EW of 210 mÅ even without an enhanced EUV over-ionisation of He I. Such models could be consistent with the scenario suggested by Sanz-Forcada & Dupree (2008) in which the He triplet is controlled by EUV photons amongst low-activity dwarfs, but becomes progressively governed by collisional processes in higher activity dwarfs, for which the active regions may be constituted of higher density plasma than active regions on low-activity stars. Since the collisionally excited λ1549 multiplet of C IV (San-Forcada & Dupree 2008) does seem to scale with the He I λ10830 triplet (Figure 6), this could add evidence for collisional influence on the He triplet.

Vieytes, Mauas, & Cincunegui (2005) and Vieytes, Mauas, & Díaz (2009) used the chromospheric structure models of Fontenla, Avrett, & Loeser (1993) to match observed spectrum profiles of the Hβ, Ca II K, Mg I b, and Na D lines in a sample of G and K dwarfs with various levels of stellar activity. Models that best matched the spectra have a characteristic that the mass column density corresponding to the base of the TR increases with increasing Ca II K-line emission. The temperature profile in the chromosphere of a high-activity G or K dwarf with strong Ca II emission was found to be shifted inwards to deeper column and mass densities than in a lower activity dwarf with weaker K emission (see also Andretta & Giampapa 1995 who further argue that this will be accompanied by increasing densities in the corona). Such a trend is in accord with earlier models such as those of Kelch, Worden, & Linsky (1979), as well as the arguments of Sanz-Forcada & Dupree (2008) that the He I triplet line is formed in a higher density environment in active chromospheres.

Coronal temperatures are greater in high-activity stars than in solar active regions (e.g., Drake et al. 2000). However, the observation that some dwarfs with similar X-ray Hardness Ratios HR1 and HR2 can have different strengths of the λ10830 line (Figure 4), further suggests that temperature of the corona alone is not the only factor governing the formation of this triplet feature. Rather the entire temperature-density structure of the chromosphere, TR, and lower corona, or at least the active regions within them, may differ between dwarfs with strong and weak He I triplet lines, as in the models of Andretta & Giampapa (1995). This would be consistent with the tendency for the triplet strength to correlate with a variety of chromosphere/TR/corona emission measures. Vieytes et al. (2009) concluded that since the chromosphere moves deeper in more-active G and K dwarfs, the site of energy deposition that heats the chromosphere is also located deeper within the atmospheres of such stars.

Correlations between He I triplet EW and the various stellar activity indicators employed in this paper break down amongst dwarfs with $(B-V) < 0.47$, i.e., amongst dwarfs earlier than spectral type F6. Zarro & Zirin (1986) proposed that this contrast corresponds with a difference between early-F and late-F dwarfs in magnetic dynamo behaviour, the driver of stellar activity in solar-type stars. One possibility which they suggested, based on the work of Giampapa & Rosner (1984), is that shallower outer convection zones of early-F dwarfs are not conducive to the formation of large magnetic flux tubes, with the result that 'a more uniform surface distribution of enhanced magnetic flux is expected in the early dF stars' than on the quiet Sun. Simon & Drake (1989) noted that amongst F and G dwarfs the cooler stars manifest more of a trend between stellar activity proxies than do the hotter F dwarfs. Consequently, the lack of a correlation between He I EW and coronal/TR/chromospheric emission amongst the earliest F stars may be linked to non-correlations between other pairs of activity tracers. Simon & Drake (1989) discussed at some length the possible differences in activity between early-F and late-F dwarfs. They suggested that the chromospheres of early-F dwarfs are a product of acoustic heating, whereas a magnetic dynamo is responsible in late-F and other solar-like dwarfs.

Alternatively, the non-correlation of He I λ10830 triplet strength with stellar activity amongst early-F dwarfs might be a consequence of the mechanism that populates the lower level of this transition. Along such lines, Zarro & Zirin (1986) proposed that electron collisional excitation of He I may increase in importance relative to the EUV-PR mechanism in early-F dwarfs, possibly because their chromospheres are hotter than those of late-F dwarfs, thereby erasing any potential correlation between λ10830 EW and coronal X-ray emission. A model along these lines might be unifiable with the suggestion of Sanz-Forcada & Dupree (2008) that collisional excitation of the triplet lower level also dominates in the chromospheres of highly active late-F and G type dwarfs that have enhanced λ10830 lines.

The He I data sets on which this paper is based are still relatively spartan. Much could be done to repeat and expand upon the Zarro & Zirin (1986) survey of dwarf stars using He I λ10830 spectra of higher resolution and higher signal-to-noise (S/N), in order to more precisely define the amount of intrinsic scatter in correlations such as those of Figures 2 and 5. It could be beneficial to preselect a sample of several hundred FGK dwarfs for which coronal soft X-ray measurements of L_x/L_{bol} are available from the *ROSAT*, *Chandra*, or *XMM-Newton* spacecraft observatories. Alternatively, measurements have been published in the literature of the chromospheric Ca II H and K emission for thousands of dwarf stars that could serve as a sample to map out the fine structure of Figure 5. Stars selected to encompass the full range in L_x/L_{bol} and R'_{HK} that exists amongst solar neighourhood dwarfs would allow the behaviour of the He I line to be more fully documented at the highest levels of activity, as well as amongst very low-activity dwarfs in analogs to Maunder-minimum states. Samples could also be comprised of dwarfs for which *IUE* or *HST* ultraviolet spectroscopy is available of TR emission lines, in order to better define the trends noted in Figures 6 and 7. Such surveys could eventually document how the He I λ10830 line varies with stellar age, as well as impose constraints on the formation process of the line, via the arguments of, for example, Sanz-Forcada & Dupree (2008). It would also be worthwhile to include dwarfs with a significant range in [Fe/H] in order to cover a range of metallicity, which can serve as another pseudo-proxy for age.

Surveys such as those suggested in the previous paragraph would involve comparing He I triplet spectroscopy with other activity data acquired at different epochs. Such comparisons, however, make it difficult to take account of intrinsic variability in the He I line strength. Both the chromospheric and coronal emission of the Sun vary with the solar activity cycle. Monitoring of photometric magnitudes and the R'_{HK} index has shown that chromospheric activity cycles are common amongst FGK dwarf stars (e.g., Wilson 1978; Baliunas & Vaughan 1985; Baliunas et al. 1995, 1996b; Lockwood et al. 2007; Oláh et al. 2009), so it seems likely that the He I EW

will also prove to be variable amongst them. Spectroscopic monitoring of the He I EW might provide a tool for searching for coronal activity cycles amongst late-type dwarfs, should high-(S/N) data be capable of detecting intrinsic variations in EW at a level of ∼10 mÅ or better. Simultaneous spectroscopy of the He I λ10830 and Ca II H and K emission lines over many years may be able to map out correlations between coronal and chromospheric activity through entire stellar activity cycles. Such data-intensive programmes might be less feasible if spacecraft data have to be depended upon for coronal information.

ACKNOWLEDGEMENTS

This research has made use of the SIMBAD database, operated at CDS, Strasbourg, France. The author gratefully acknowledges the support of award AST-1517791 from the National Science Foundation of the United States. We thank Gustavo Porto de Mello for a very collegial referee's report.

REFERENCES

Andretta, V., & Giampapa, M. S. 1995, ApJ, 439, 405
Andretta, V., & Jones, H. P. 1997, ApJ, 489, 375
Athey, R. G., & Johnson, H. R. 1960, ApJ, 131, 413
Avrett, E. H., Fontenla, J. M., & Loeser, R. 1994, in IAU Symp., Infrared Solar Physics, eds. D. M. Rabin, J. T. Jefferies, & C. Lindsey (Dordrecht: Kluwer), 35
Ayres, T. R., Marstad, N. C., & Linsky, J. L. 1981, ApJ, 247, 545
Baliunas, S., Sokoloff, D., & Soon, W. 1996a, ApJ, 457, L99
Baliunas, S. L., Nesme-Ribes, E., Sokoloff, D., & Soon, W. H. 1996b, ApJ, 460, 848
Baliunas, S. L., & Vaughan, A. H. 1985, ARA&A, 23, 379
Baliunas, S. L., et al. 1995, ApJ, 438, 269
Beardsley, W. R., Gatewood, G., & Kamper, K. W. 1974, ApJ, 194, 637
Bianchi, L. 2014, ApSS, 354, 103
Boksenberg, A., et al. 1973, MNRAS, 163, 291
Bopp, B. W., & Fekel, F. C. 1977, AJ, 82, 490
Carr, M. J., Meurs, E. J. A., & Cunniffe, J. 2004, in Astronomical Data Analysis III, Electronic Workshops in Computing, British Computer Society, Session 2, paper 7, http://www.bcs.org/upload/pdf/ewic-ada04-s2paper7.pdf
Centeno, R., Trujillo Bueno, J., Uitenbroek, H., & Callados, M. 2008, ApJ, 677, 742
Dempsey, R. C., Linsky, J. L., Fleming, T. A., & Schmitt, J. H. M. M. 1993, ApJS, 86, 599
de Toma, G., Holzer, T. E., Burkepile, J. T., & Gilbert, H. R. 2005, ApJ, 621, 1109
Drake, J. J., Peres, G., Orlando, S., Laming, J. M., & Maggio, A. 2000, ApJ, 545, 1074
Dupree, A. K., Penn, M. J., & Jones, H. P. 1996, ApJ, 467, L121
Eker, Z. 1992, ApJS, 79, 481
Fernández-Figueroa, M. J., Montes, D., De Castro, E., & Cornide, M. 1994, ApJS, 90, 433
Findheisen, K., Hillenbrand, L., & Soderblom, D. 2011, AJ, 142, 23
Flower, P. J. 1996, ApJ, 469, 355
Fontenla, J., Avrett, E., & Loeser, R. 1993, ApJ, 406, 319
Giampapa, M. S., & Rosner, R. 1984, ApJ, 286, L19
Giovanelli, R. G., Hall, D. N. B., & Harvey, J. W. 1972, SoPh, 22, 53
Gondoin, P. 2013, A&A, 556, A14
Gray, R. O., Corbally, C. J., Garrison, R. F., McFadden, M. T., Bubar, E. J., McGahee, C. E., O'Donoghue, A. A., & Knox, E. R. 2006, AJ, 132, 161
Gray, R. O., Corbally, C. J., Garrison, R. F., McFadden, M. T., & Robinson, P. E. 2003, AJ, 126, 2048
Haisch, B. M., & Basri, G. 1985, ApJS, 58, 179
Hall, D. S. 1976, in IAU Colloq., 29, Multiply Periodic Phenomena in Variable Stars, ed. W. S. Fitch (Dordrecht: Reidel), 287
Hall, J. C., Henry, G. W., Lockwood, G. W., Skiff, B. A., & Saar, S. H. 2009, AJ, 138, 312
Harvey, J. W., & Livingston, W. C. 1994, in IAU Symp., Infrared Solar Physics, eds. D. M. Rabin, J. T. Jefferies, & C. Lindsey (Dordrecht: Kluwer), 59
Harvey, J. W., & Sheeley, N. R., Jr 1977, SoPh, 54, 343
Henry, T. J., Soderblom, D. R., Donahue, R. A., & Baliunas, S. L. 1996, AJ, 111, 439
Hünsch, M., Schmitt, J. H. M. M., & Voges, W. 1998, A&AS, 132, 155
Isaacson, H., & Fischer, D. 2010, ApJ, 725, 875
Jenkins, J. S., Jones, H. R. A., Pavlenko, Y., Pinfield, D. J., Barnes, J. R., & Lyubchik, Y. 2008, A&A, 485, 571
Jenkins, J. S., et al. 2006, MNRAS, 372, 163
Jordan, C., Ayres, T. R., Brown, A., Linsky, J. L., & Simon, T. 1987, MNRAS, 225, 903
Kastner, J. H., Crigger, L., Rich, M., & Weintraub, D. A. 2003, ApJ, 585, 878
Katsova, M. M., & Livshits, M. A. 2011, ARep, 55, 1123
Kelch, W. L., Worden, S. P., & Linsky, J. L. 1979, ApJ, 229, 700
Lanzafame, A. C., & Byrne, P. B. 1995, A&A, 303, 155
Linsky, J. L., Bushinsky, R., Ayres, T., Fontenla, J., & France, K. 2012, ApJ, 745, 25
Lites, B. W., Keil, S. L., Scharmer, G. B., & Wyller, A. A. 1985, SoPh, 97, 35
Lockwood, G. W., Skiff, B. A., Henry, G. W., Henry, S., Radick, R. R., Baliunas, S. L., Donahue, R. A., & Soon, W. 2007, ApJS, 171, 260
Makarov, V. V. 2003, AJ, 126, 1996
Malanushenko, O. V., & Jones, H. P. 2005, SoPh, 226, 3
Martin, D. C., et al. 2005, ApJ, 619, L1
Mermilliod, J. -C., Mermilliod, M., & Hauck, B. 1997, A&AS, 124, 349
Meurs, E. J. A., Casey, P., & Norci, L. 2003, AN, 324, 146
Meurs, E. J. A., Casey, P., & Norci, L. 2006, in IAU Symp., Vol.230, Populations of High Energy Sources in Galaxies, eds. E. J. A. Meurs, & G. Fabbiano (Cambridge: Cambridge University Press), 45
Morossi, C., Franchini, M., Malagnini, M. L., & Chavez, M. A. 2003, in Proc. 12th Cambridge Workshop on Cool Stars, Stellar Systems, and the Sun, eds. A. Brown, G. H. Harper, & T. R. Ayres (Boulder, CO: Univ. Colorado), 285
Morrissey, P., et al. 2005, ApJ, 619, L7
Neuhaeuser, R., Sterzik, M. F., Schmitt, J. H. M. M., Wichmann, R., & Krautter, J. 1995, A&A, 297, 391
Noyes, R. W., Hartmann, L. W., Baliunas, S. L., Duncan, D. K., & Vaughan, A. H. 1984, ApJ, 279, 763
O'Brien, G. T., Jr, & Lambert, D. L. 1986, ApJS, 62, 899
Oláh, K., et al. 2009, A&A, 501, 703

Osten, R. A., & Brown, A. 1999, ApJ, 515, 746
Pace, G. 2013, A&A, 551, L8
Pizzolato, N., Maggio, A., Micela, G., Sciortino, S., & Ventura, P. 2003, A&A, 397, 147
Ramírez, I., & Meléndez, J. 2005, ApJ, 626, 465
Raymond, J. C., & Smith, B. S. 1977, ApJS, 35, 419
Rocha-Pinto, H. J., & Maciel, W. J. 1998, MNRAS, 298, 332
Santos, N. C., et al. 2011, A&A, 526, 112
Sanz-Forcada, J., Brickhouse, N. S., & Dupree, A. K. 2002, ApJ, 570, 799
Sanz-Forcada, J., & Dupree, A. K. 2008, A&A, 488, 715
Schroeder, C., Reiners, A., & Schmitt, J. H. M. M. 2009, A&A, 493, 1099
Simon, T., & Drake, S. A. 1989, ApJ, 346, 303
Smith, G. H., Dupree, A. K., & Günther, H. M. 2016, AJ, 152, 43
Smith, G. H., Dupree, A. K., & Strader, J. 2012, PASP, 124, 1252
Smith, G. H., & Redenbaugh, A. K. 2010, PASP, 122, 1303
Smith, G. H., Redenbaugh, A. K., & Jones, A. 2011, Obs, 131, 1
Smith, M. A. 1983, ApJ, 88, 1031
Soderblom, D. R. 1985, AJ, 90, 2103
Soderblom, D. R., Duncan, D. K., & Johnson, D. R. H. 1991, ApJ, 375, 722
Soon, W. H., Zhang, Q., Baliunas, S. L., & Kurucz, R. L. 1993, ApJ, 416, 787
Strassmeier, K. G., Hall, D. S., Zeilik, M., Nelson, E., Eker, Z., & Fekel, F. C. 1988, A&AS, 72, 291
Takeda, Y., & Takada-Hidai, M. 2011, PASJ, 63, 547
Thompson, G. I., Nandy, K., Jamar, C., Monfils, A., Houziaux, L., Carnochan, D. J., & Wilson, R. 1978, Catalogue of Stellar Ultraviolet Fluxes *(TD-1)*: A Compilation of Absolute Stellar Fluxes Measured by the Sky Survey Telescope (S2/68) Aboard the ESRO Satellite *TD-1*, The Science Research Council, United Kingdom
VandenBerg, D. A., & Poll, H. E. 1989, AJ, 98, 1451
van Leeuwen, F. 2007, A&A, 474, 653
Vaughan, A. H., & Preston, G. W. 1980, PASP, 92, 385
Vaughan, A. H., Preston, G. W., & Wilson, O. C. 1978, PASP, 90, 267
Vaughan, A. H., Jr, & Zirin, H. 1968, ApJ, 152, 123
Vernazza, J. E., Avrett, E. H., & Loesser, R. 1976, ApJS, 30, 1
Vernazza, J. E., Avrett, E. H., & Loesser, R. 1981, ApJS, 45, 635
Vican, L. 2012, AJ, 143, 135
Vieytes, M. C., Mauas, P. J. D., & Cincunegui, C. 2005, A&A, 441, 701
Vieytes, M. C., Mauas, P. J. D., & Díaz, R. F. 2009, MNRAS, 398, 1495
Voges, W., et al. 1999, A&A, 349, 389
Wenger, M., et al. 2000, A&AS, 143, 9
Wilson, O. C. 1978, ApJ, 226, 379
Wright, J. T. 2004, AJ, 128, 1273
Wright, J. T., Marcy, G. W., Butler, R. P., & Vogt, S. S. 2004, ApJS, 152, 261
Wright, N. J., Drake, J. J., Mamajek, E. E., & Henry, G. W. 2011, ApJ, 743, 48
Wright, N. J., Drake, J. J., Mamajek, E. E., & Henry, G. W. 2013, AN, 334, 151
Zarro, D. M., & Zirin, H. 1986, ApJ, 304, 365
Zeng, Z., Qiu, J., Cao, W., & Judge, P. G. 2014, ApJ, 793, 87
Zirin, H. 1975, ApJ, 199, L63
Zirin, H. 1982, ApJ, 260, 655